

Electron-phonon coupling in cuprate high-temperature superconductors determined from electron relaxation rates

C. Gadermaier,¹ A. S. Alexandrov,^{2,1} V. V. Kabanov,¹ P. Kusar,¹ T. Mertelj,¹ X. Yao,³ C. Manzoni,⁴ D. Brida,⁴ G. Cerullo,⁴ and D. Mihailovic^{1,*}

¹*Jozef Stefan Institute, 1000 Ljubljana, Slovenia*

²*Department of Physics, Loughborough University, Loughborough LE11 3TU, United Kingdom*

³*Department of Physics, Shanghai Jiao Tong University, Shanghai 200240, China*

⁴*National Laboratory for Ultrafast and Ultraintense Optical Science, INFN-CNR, Dipartimento di Fisica, Politecnico di Milano, 20133 Milano, Italy*

The electronic relaxation times are determined via pump-probe optical spectroscopy using sub-15 fs pulses over a wide range of probe energies for the normal state of two different cuprate superconductors. We show that the primary relaxation process is electron-phonon scattering, in contrast to the basic assumptions of the two-temperature model, which is conventionally used to describe electron relaxation in metals and related materials. Based on the exact analytic solution for the electron relaxation, we extract values for the second moments of the Eliashberg functions $\lambda\langle\omega^2\rangle = 800 \pm 200 \text{ meV}^2$ for $\text{La}_{1.85}\text{Sr}_{0.15}\text{CuO}_4$ and $\lambda\langle\omega^2\rangle = 400 \pm 100 \text{ meV}^2$ for $\text{YBa}_2\text{Cu}_3\text{O}_{6.9}$. These values are consistent with a phonon-mediated polaronic pairing mechanism.

PACS numbers: 78.47.J-, 74.72.-h, 42.65.Re, 71.38.-k

The electron-phonon interaction (EPI) is decisive for determining the functional properties of materials. It is a main scattering process in electron conduction and is vital for the formation of ordered electronic states such as charge-density waves and often the superconducting condensate. The determination of its strength $\lambda\langle\omega^2\rangle$ from phonon linewidths in Raman and neutron scattering is often compromised by selection rules and inhomogeneous broadening. Hence, the most accurate estimate is from electron relaxation times τ . To date, a theoretical expression of τ in terms of $\lambda\langle\omega^2\rangle$ has been provided by the two-temperature model (TTM)[1, 2], which describes the relaxation of a quasi-equilibrium distribution of electrons. The TTM is based on the assumption that the relaxation time due to electron-electron (e-e) collisions τ_{e-e} is much shorter than the electron-phonon (e-ph) relaxation time τ_{e-ph} . Recently, an exact analytic solution has been derived without any a priori assumption about the relative values of τ_{e-e} and τ_{e-ph} [3], which opens the possibility to analyze experimental data in systems with strong EPI.

In this paper we study the electron relaxation in two high- T_c cuprate superconductors, where EPI is expected to be strong. To eliminate any interference due to emerging low temperature order, like pseudogap, antiferromagnetic, or stripe phases, we perform all experiments at room temperature. Since strong EPI leads to short relaxation times, we use a non-standard femtosecond laser setup with sub-15 fs pulses, in order to improve the time resolution compared to previous experiments. We show that our experimental results both quantitatively and qualitatively contradict the TTM. Hence we use the more accu-

rate description from[3]. The obtained $\lambda\langle\omega^2\rangle = 400 \pm 100 \text{ meV}^2$ for $\text{YBa}_2\text{Cu}_3\text{O}_{6.9}$ and $\lambda\langle\omega^2\rangle = 800 \pm 200 \text{ meV}^2$ for $\text{La}_{1.85}\text{Sr}_{0.15}\text{CuO}_4$ demonstrate that the EPI is strong enough to have a crucial role in the high- T_c superconductivity mechanism.

In femtosecond optical pump-probe spectroscopy the sample is excited with a short pump laser pulse, and the relative photoinduced reflectivity change $\Delta R/R$ is measured with a (weaker) probe pulse at a variable delay t . We used 15-fs pump pulses centred at 530 nm and broad band sub-10-fs probe pulses with a spectrum ranging from 500 to 700 nm, from two synchronised broad-band non-collinear optical parametric amplifiers (NOPAs). This non-degenerate pump-probe configuration eliminates coherent interference artifacts. The working principles of NOPAs and pulse compression are described in[4]. Single crystals of $\text{YBa}_2\text{Cu}_3\text{O}_{6.9}$ and $\text{La}_{1.85}\text{Sr}_{0.15}\text{CuO}_4$ were prepared as in[5, 6]. Details about the experimental and theoretical methods are given in the supplementary material.

Two-dimensional maps of the photoinduced $\Delta R/R$ as a function of probe wavelength and delay are shown for both materials in Figure 1. In both samples there is a fast initial decay followed by a slower dynamics, which for some wavelengths has opposite sign. Additionally, the $\text{YBa}_2\text{Cu}_3\text{O}_{6.9}$ signal bears a strong contribution from coherent phonons. Time traces at selected wavelengths (integrated over a 10-15 nm spectral window) are depicted in Figure 2. For different pump intensities the dynamics does not change and the signal magnitude increases almost linearly. We fit the transient response of both samples with two exponential decay components with time constants τ_a and τ_b , and a long-lived plateau, using the pump-probe cross-correlation as the generation term. For each sample, the same τ_a and τ_b are used for the whole spectral range. The fit yields $\tau_a = 45 \pm 8 \text{ fs}$ and $\tau_b = 600 \pm 100 \text{ fs}$ for $\text{La}_{1.85}\text{Sr}_{0.15}\text{CuO}_4$ and $\tau_a = 100 \pm 20$

*Correspondence and request for materials should be addressed to Dragan Mihailovic. e-mail: dragan.mihailovic@ijs.si

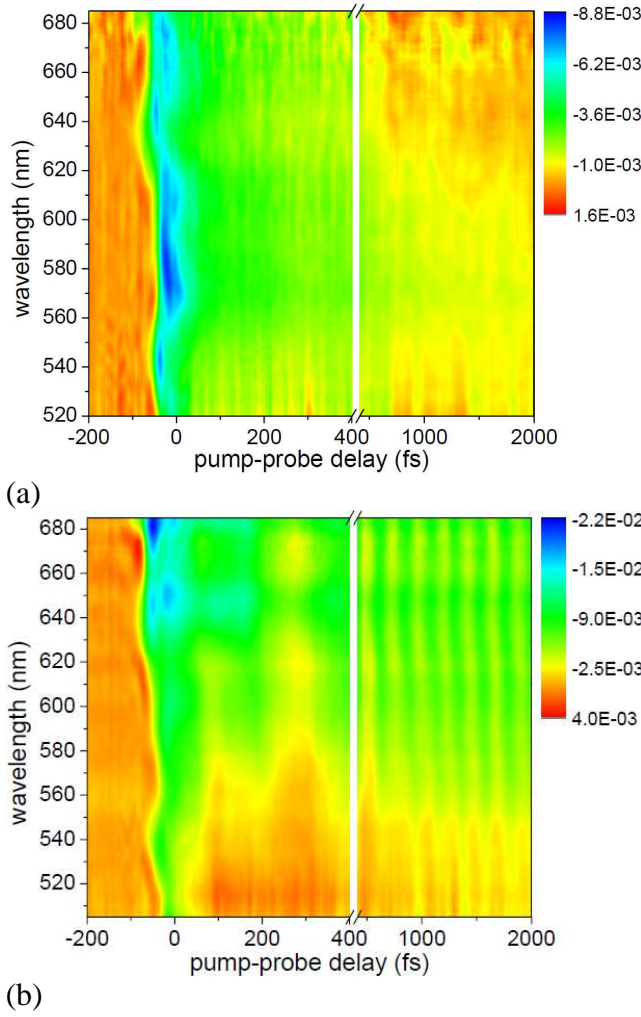


Figure 1: Transient photoinduced reflectivity change $\Delta R/R$ of $\text{La}_{1.85}\text{Sr}_{0.15}\text{CuO}_4$ (a) and $\text{YBa}_2\text{Cu}_3\text{O}_{6.9}$ (b) at a pump intensity of $200 \mu\text{J}/\text{cm}^2$.

fs and $\tau_b = 450 \pm 100$ fs for $\text{YBa}_2\text{Cu}_3\text{O}_{6.9}$.

In the linear approximation $\Delta R/R$ directly tracks the electronic relaxation processes, and τ_a and τ_b are the characteristic times of two electron relaxation processes. This approximation is justified by two essential characteristics of our data: (i) the $\Delta R/R$ amplitude is linear in the excitation intensity, and (ii) the same decay times appear independently of the probe wavelength (see Figure 2a for $\text{La}_{1.85}\text{Sr}_{0.15}\text{CuO}_4$), only with different spectral weights of the individual components. Following previous studies[7, 8] as well as for reasons given below, we assign τ_a to relaxation via the EPI. The origin of the longer relaxation time τ_b has been discussed in detail previously[6–9] and is of no further interest here.

Historically, an analytical expression that links EPI to the electron relaxation time has been obtained in the framework of the TTM[1, 2]. It is based on the assumption that e-e scattering should establish a thermal distribution of electrons with a temperature $T_e > T_l$ (T_l

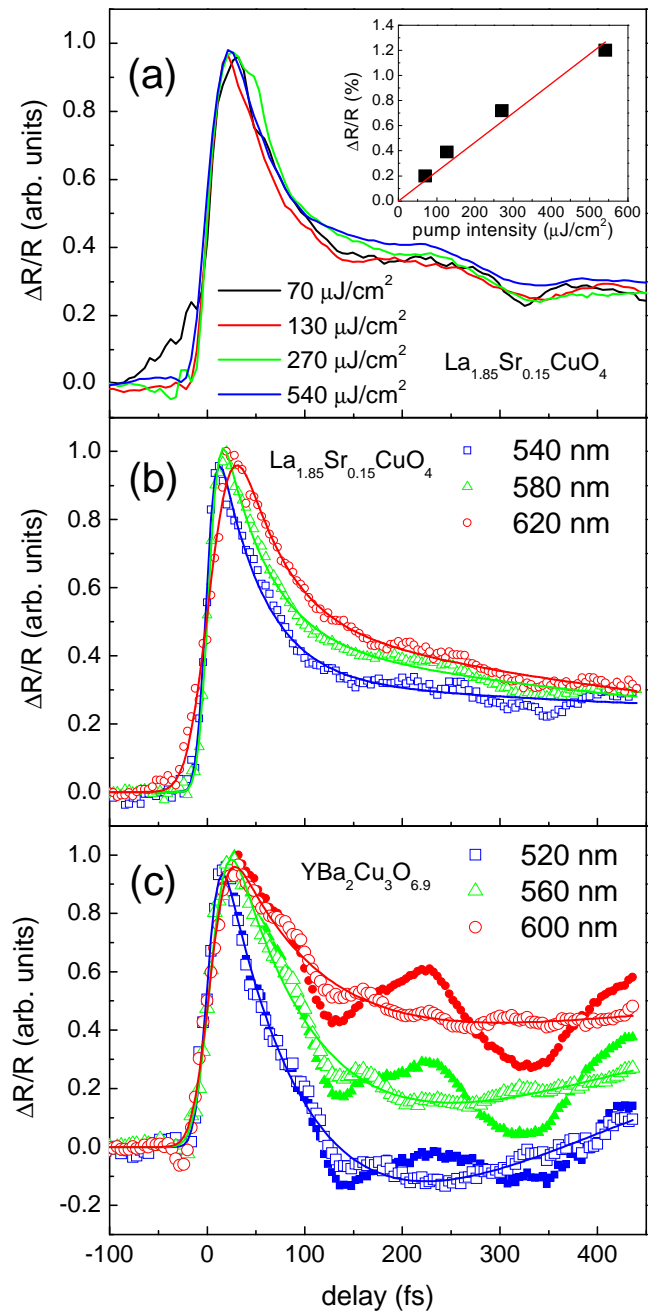


Figure 2: a) Normalised photoinduced reflectivity change in $\text{La}_{1.85}\text{Sr}_{0.15}\text{CuO}_4$ at 590 nm for different pump intensities. The inset shows the signal magnitude as a function of pump intensity. b) $\Delta R/R$ of $\text{La}_{1.85}\text{Sr}_{0.15}\text{CuO}_4$ at different probe wavelengths (symbols) and double-exponential fits (lines). c) $\Delta R/R$ of $\text{YBa}_2\text{Cu}_3\text{O}_{6.9}$ at different probe wavelengths and double-exponential fits. Small full symbols show the original data, large open symbols show the data after subtraction of three oscillating modes at 115, 145, and 169 cm^{-1} , which are known from Raman spectroscopy [10, 11].

being the lattice temperature) on a time scale typically faster than the experimental time resolution. The relaxation time τ_{e-ph} of subsequent cooling via EPI is related to the second moment of the Eliashberg spectral function $\lambda\langle\omega^2\rangle = \pi k_B T_e / 3\hbar\tau_{e-ph}$. This estimate has been used in the analysis of optical fs experiments[8, 12], and recently also fs transient angle-resolved photoemission spectroscopy (ARPES)[7].

Let us now assess the applicability of the TTM to our data. In the weak photoexcitation regime where only a small fraction of conduction electrons is excited ($k_B T_e \ll E_F$), e-e scattering is impeded since the Pauli exclusion principle strongly limits the number of available final states. The e-e relaxation time τ_{e-e} can be estimated by: $1/\tau_{e-e} \approx \pi^3 \mu_c^2 (k_B T_e)^2 / 4\hbar E_F$ (see [3] and the supplementary information for details), where $\mu_c = r_s / 2\pi$ is the Coulomb pseudopotential characterising the electron-electron interaction. Even in the weak photoexcitation regime, the effective T_e after excitation can differ significantly from room temperature. Assuming an electronic specific heat of 1.4 mJ/g.at.K² [13], and a pump laser penetration depth of 150 nm, one can estimate $T_e = 400$ K, $\tau_{e-e} \approx 1.5$ ps for the lowest and $T_e = 800$ K, $\tau_{e-e} \approx 370$ fs for the highest pump fluence used in Fig. 2a. Even the lowest estimate for τ_{e-e} clearly rules out both the traditional assumption $\tau_{e-e} \ll \tau_a$ and the possibility $\tau_a = \tau_{e-e}$, i.e. that we actually observe e-e scattering. Moreover, in the TTM τ_{e-e} and τ_{e-ph} should scale with the fluence dependent effective electron temperature, as T_e^{-2} and T_e , respectively, contrary to the observed fluence independence of τ_a (See Fig. 2a). Therefore, the only remaining scenario is that $\tau_a < \tau_{e-e}$, in which case the TTM is clearly no longer appropriate to describe the fast relaxation dynamics in our compounds.

Outside the TTM regime, the relaxation behavior can be described via the kinetic Boltzmann equation using e-e and e-ph collision integrals. This has been done both numerically[14] and analytically[3, 15]. In the supplementary information we show how the analytical solution yields an expression for the time dependence of the electron energy, which describes the measured electron energy distribution by ARPES better than the TTM (see supplementary Figure 6). The electron relaxation can be approximated with an exponential decay where the time constant $\tau_a = \tau_{e-ph}$ turns out to be twice the TTM relaxation time (see supplementary Figure 4):

$$\lambda\langle\omega^2\rangle = \frac{2\pi}{3} \frac{k_B T_l}{\hbar\tau_{e-ph}}. \quad (1)$$

Using this more accurate expression we can now give better estimates for the EPI in cuprate superconductors. The obtained relaxation times $\tau_a \approx 45 \pm 8$ fs for La_{1.85}Sr_{0.15}CuO₄ and $\tau_a \approx 100 \pm 20$ fs for YBa₂Cu₃O_{6.9} the yield $\lambda\langle\omega^2\rangle = 800 \pm 200$ meV² and $\lambda\langle\omega^2\rangle = 400 \pm 100$ meV², respectively.

The main qualitative difference between our model and the TTM is that Eq. 1 contains T_l , which is close to room temperature and, consistent with our experimental

findings, shows almost no fluence dependence due to the higher heat capacity of the lattice, while the TTM uses T_e , which for typical fluences is a few hundred K higher (see e.g.[16] for a number of conventional superconductors). Hence, *by coincidence*, in the literature T_e is often close to $2T_l$, which approximately cancels with the factor 2 between our and the TTM equations. Thus a revision of the literature values of $\lambda\langle\omega^2\rangle$ using our model will often yield very similar results as the TTM. The important difference between the two models is that the TTM predicts a strongly fluence dependent relaxation time, which to the best of our knowledge has never been observed. On the other hand, a linear increase of τ_{e-ph} with T_l , as predicted by Eq. 1, has been observed [17, 41].

We have shown how the appropriate theory and the necessary temporal resolution allow the determination of accurate values for $\lambda\langle\omega^2\rangle$ even in the case of strong EPI. Let us now assess the possible contribution of EPI to the superconductive pairing mechanism in the cuprates, based on the experimental values we obtain for YBa₂Cu₃O_{6.9} and La_{1.85}Sr_{0.15}CuO₄. The most common expression that relates EPI to T_c is the BCS-McMillan formula $k_B T_c = \hbar\omega_0 \exp[-(1+\lambda)/\lambda]$ (if any repulsive Coulomb pseudopotential is neglected), where ω_0 is a characteristic phonon frequency. For any *fixed* $\lambda\langle\omega^2\rangle$ we can write $k_B T_c = \hbar\sqrt{\lambda\langle\omega^2\rangle/\lambda} \exp[-(1+\lambda)/\lambda]$ and find a maximum for $T_c(\lambda)$ at $\lambda = 2$. For our experimental values of $\lambda\langle\omega^2\rangle$, we obtain maximum critical temperatures $T_c^{max} = 52$ K for La_{1.85}Sr_{0.15}CuO₄ and $T_c^{max} = 37$ K for YBa₂Cu₃O_{6.9}. Clearly BCS theory cannot account for T_c of YBa₂Cu₃O_{6.9}. More remarkably, contrary to the experiment, it predicts a higher T_c for La_{1.85}Sr_{0.15}CuO₄ than for YBa₂Cu₃O_{6.9}.

A more accurate estimate of λ requires a detailed knowledge of the Eliashberg spectral function. This can be extracted from other experiments such as optical absorption[18, 19], neutron scattering[20–22], ARPES[23, 24], and tunnelling[25–30]. Based on these references the best estimate of ω_0 is about 40 meV or less, which gives $\lambda \gtrsim 0.5$ for La_{1.85}Sr_{0.15}CuO₄ and $\lambda \gtrsim 0.25$ for YBa₂Cu₃O_{6.9}, which give even lower BCS values for T_c . Remarkably, these λ values agree very well with ab initio calculations that predict 0.27 for YBa₂Cu₃O_{6.9}[31] and 0.4 for La_{1.85}Sr_{0.15}CuO₄[32].

From the above considerations we can formulate the prerequisites for a theory that describes the pairing through EPI. (i) It yields a maximum $T_c(\lambda)$ that is significantly higher than for BCS and (ii) this maximum is obtained around the λ value for YBa₂Cu₃O_{6.9} and clearly below the λ for La_{1.85}Sr_{0.15}CuO₄. Both conditions point to the polaronic mechanism of pairing[33–36]. The highest $T_c(\lambda)$ exceeding the BCS value by several times is found in the intermediate crossover region of the EPI strength, $\lambda_c \approx 1$ from the weak-coupling BCS to the strong-coupling polaronic superconductivity. Strong electron-electron correlations shift the crossover region to smaller values of λ_c [37, 38] ($\lambda_c \approx 0.9$ for uncorrelated 2D polarons[39], while $\lambda_c \lesssim 0.4$ in the Holstein t-J

model[38]). Our results suggest that $\text{YBa}_2\text{Cu}_3\text{O}_{6.9}$ is in the crossover region, while $\text{La}_{1.85}\text{Sr}_{0.15}\text{CuO}_4$ is on the strong-coupling side of this region ($\lambda > \lambda_c$).

Compared to a simple FL, e-e correlations increase the effective mass of carriers (or decrease the bare bandwidth), and heavier carriers form lattice polarons at a smaller value of λ . Both spin and lattice polarons have the same Fermi surface as free electrons, but the Fermi energy is reduced[40]. Our (Boltzmann) relaxation theory is based on the existence of the Fermi surface and the Pauli exclusion principle, which the dressed (polaronic) carriers obey like free electrons. Therefore, Equation 1 and all our subsequent considerations are valid also for polarons in the presence of strong electron correlations.

While we do not exclude any non-phononic contribution to the pairing, our direct measurement result brings into focus the other compelling experimental evidence for a strong EPI obtained from isotope effects[25], high resolution ARPES[23, 24], optical[18, 19], neutron-scattering[20–22], and tunnelling [29, 30, 42] spectroscopies.

In our study on cuprates we demonstrate how to deter-

mine accurate values for $\lambda\langle\omega^2\rangle$ by using the appropriate theory and adequate time resolution. Similar work will be of fundamental significance for other effects where EPI is important, such as high T_c superconductivity in other materials (notably iron-pnictides[41]), colossal magnetoresistance, charge density waves, or polaron formation.

Acknowledgments

This work was supported by the Slovenian Research Agency (ARRS) (grants 430-66/2007-17 and BI-CN/07-09-003), EPSRC (UK) and the Royal Society (grants EP/D035589/1 and JP090316), MOST of China (Project 2006CB601003), and by the European Commission (grants EIF-040958A, ERG-230975, and the European Community Access to Research Infrastructure Action, Contract RII3-CT-2003-506350 (Centre for Ultrafast Science and Biomedical Optics, LASERLAB-EUROPE)). We thank S. Sugai for the $\text{La}_{1.85}\text{Sr}_{0.15}\text{CuO}_4$ sample and D. Polli and for fruitful discussions.

-
- [1] M. I. Kaganov, I. M. Lifshits, and L. B. Tanatarov, *Zh. Eksp. Teor. Fiz.* **31**, 232, (1956) [*Sov.Phys. JETP* **4**, 173 (1957)].
- [2] P. B. Allen, *Phys. Rev. Lett.* **59**, 1460 (1987).
- [3] V. V. Kabanov and A. S. Alexandrov, *Phys. Rev. B* **78** 174514 (2008).
- [4] C. Manzoni, D. Polli, and G. Cerullo, *Rev. Sci. Instrum.* **77**, 023103 (2006).
- [5] H. Gao *et al.*, *Phys. Rev. B* **74** 020505(R) (2006).
- [6] P. Kusar *et al.*, *Phys. Rev. Lett.* **101**, 227001 (2008).
- [7] L. Perfetti *et al.*, *Phys. Rev. Lett.* **99**, 197001 (2007).
- [8] J.-X. Zhu *et al.*, arXiv:0806.2664. (2008).
- [9] V. V. Kabanov, J. Demsar, B. Podobnik, and D. Mihailovic, *Phys. Rev. B* **59**, 1497 (1999).
- [10] E. T. Heyen *et al.*, *Phys. Rev. Lett.* **65**, 3048 (1990).
- [11] M. N. Iliev *et al.*, *Phys. Rev. B* **77**, 174302 (2008).
- [12] S. V. Chekalin *et al.*, *Phys. Rev. Lett.* **67**, 3860 (1991).
- [13] J. W. Loram, K. A. Mirza, J. R. Cooper, and W. Y. Liang, *Phys. Rev. Lett.* **71**, 1740 (1993).
- [14] R. H. M. Groeneveld, R. Sprik, and A. Lagendijk, *Phys. Rev. B* **51**, 11433 (1995).
- [15] V. E. Gusev and O. B. Wright, *Phys. Rev. B* **57**, 2878 (1998).
- [16] S. D. Brorson *et al.*, *Phys. Rev. Lett.* **64**, 2172 (1990).
- [17] Y. H. Liu *et al.*, *Phys. Rev. Lett.* **101**, 137003 (2008).
- [18] D. Mihailovic, C. M. Foster, K. Voss, and A. J. Heeger, *Phys. Rev. B* **42**, 7989 (1990).
- [19] R. Zamboni, G. Ruani, A. J. Pal, and C. Taliani, *Solid St. Commun.* **70**, 813 (1989).
- [20] M. Arai *et al.*, *Phys. Rev. Lett.* **69**, 359 (1992).
- [21] T. Egami, *J. Low Temp. Phys.* **105**, 791 (1996).
- [22] D. Reznik *et al.*, *Nature* **440**, 1170 (2006).
- [23] A. Lanzara *et al.*, *Nature* **412**, 510 (2001).
- [24] W. Meevasana *et al.*, *Phys. Rev. Lett.* **96**, 157003 (2006).
- [25] G. M. Zhao, in *Polarons in Advanced Materials* (ed. A. S. Alexandrov, Springer, New York, 2007), vol. **103** of *Springer Series in Material Sciences*, p. 569 ; A. Bussmann-Holder and H. Keller, *ibid.*, p. 600.
- [26] S. I. Vedenev *et al.*, *Phys. Rev. B* **49**, 9823 (1994).
- [27] J. F. Zasadzinski, L. Coffey, P. Romano, Z. Yusof, *Phys. Rev. B* **68**, 180504(R) (2003).
- [28] X. J. Zhou *et al.*, *Phys. Rev. Lett.* **95**, 117001 (2005).
- [29] J. Lee *et al.*, *Nature* **442**, 546 (2006).
- [30] H. Shim, P. Chaudhari, G. Logvenov, and I. Bozovic, *Phys. Rev. Lett.* **101**, 247004 (2008).
- [31] K.-P. Bohnen, R. Heid, and M. Krauss, *Europhys. Lett* **64**, 104 (2003).
- [32] F. Giustino, m. L. Cohen, and S. G. Louie, *Nature* **452**, 975 (2008).
- [33] A. S. Alexandrov, *Zh. Fiz. Khim.* **57** 273 (1983) [*Russ. J. Phys. Chem.* **57**, 167 (1983)].
- [34] A. S. Alexandrov, *Phys. Rev. B* **38**, 925 (1988).
- [35] K. A. Müller, *J. Phys.: Condens. Matter* **19**, 251002 (2007).
- [36] T. Mertelj, V. V. Kabanov, and D. Mihailovic, *Phys. Rev. Lett.* **94**, 147003 (2005).
- [37] H. Fehske, H. Roder, G. Wellein, and A. Mitrionis, *Phys. Rev. B* **51**, 16582 (1995).
- [38] A. S. Mishchenko and N. Nagaosa, in *Polarons in Advanced Materials* (ed. A. S. Alexandrov, Springer, New York, 2007), vol. **103** of *Springer Series in Material Sciences*, p. 533.
- [39] V. V. Kabanov and O. Y. Mashtakov, *Phys. Rev. B* **47**, 6060 (1993).
- [40] A. Paramekanti, M. Randeria, and N. Trivedi, *Phys. Rev. Lett* **87**, 217002 (2001).
- [41] T. Mertelj *et al.*, arXiv:1001.1047. (2010).
- [42] G. M. Zhao, *Phys. Rev. Lett.* **103**, 236403 (2009).

Electron-phonon coupling in cuprate high-temperature superconductors determined from exact electron relaxation rates. Supplementary material.

C. Gadermaier¹, A. S. Alexandrov^{2,1}, V. V. Kabanov¹, P. Kusar¹, T. Mertelj¹, X. Yao³, C. Manzoni⁴, D. Brida⁴, G. Cerullo⁴, and D. Mihailovic¹

¹Josef Stefan Institute 1001, Ljubljana, Slovenia

²Department of Physics, Loughborough University, Loughborough LE11 3TU, United Kingdom

³Department of Physics, Shanghai Jiao Tong University,

800 Dong Chuan Road, Shanghai 200240, China

⁴National Laboratory for Ultrafast and Ultraintense Optical Science, INFM-CNR, Dipartimento di Fisica, Politecnico di Milano, 20133 Milano, Italy

A. Sample preparation

The $\text{YBa}_2\text{Cu}_3\text{O}_{6.9}$ single crystal used here was grown by top-seeded solution growth using a $\text{Ba}_3\text{Cu}_5\text{O}$ solvent(**author?**) [1]. The as-grown single crystal was first annealed at 400 °C for 180 h with flowing oxygen and slowly cooled down to room temperature. The $\text{La}_{1.85}\text{Sr}_{0.15}\text{CuO}_4$ single crystal was synthesised by a travelling-solvent-floating-zone method utilizing infrared radiation furnaces (Crystal system, FZ-T-4000) and annealed in oxygen gas under ambient pressure at 600 °C for 7 days(**author?**) [2].

B. Femtosecond pump-probe set-up

A detailed description of the set-up used is found in(**author?**) [3]. In a “pump-probe” experiment, a “pump” pulse excites the sample and the induced change in transmission or reflection of a delayed probe pulse monitors the relaxation behaviour. In order to resolve the dynamics of fast processes very short pulses are necessary, since the instrumental response function is given by the cross correlation between the pump and probe pulses. We use sub-10 fs probe pulses from an ultrabroadband (covering a spectral range from 500 to 700 nm) non-collinear optical parametric amplifier (NOPA) and ~ 15 fs pump pulses from a narrower band (wavelength tunable, in our case centred at 530 nm) NOPA. The seed pulses for the NOPAs and the amplified pulses are steered and focussed exclusively with reflecting optics to avoid pulse chirping.

A schematic of the experimental apparatus is shown in Fig. 1. The laser source is a regeneratively amplified modelocked Ti:sapphire laser (Clark-MXR Model CPA-1), delivering pulses at 1 kHz repetition rate with 780 nm center wavelength, 150 fs duration, and 500 μJ energy. Both NOPAs are pumped by the second harmonic of the Ti:sapphire laser, which is generated in a 1-mm-thick lithium triborate crystal (LBO), cut for type-I phase matching in the XY plane ($\theta = 90^\circ$, $\varphi = 31.68^\circ$, Shandong Newphotons).

The ultrabroadband visible NOPA that generates the probe pulses has been described in detail before(**author?**) [4]; a schematic of it is shown in Fig. 2. The white light continuum seed pulses are generated by a small fraction of the fundamental wavelength beam focused into a 1 mm thick sapphire plate. Parametric gain is achieved in a 1-mm-thick BBO crystal, cut at $\theta = 32^\circ$, which is the angle giving the broadest phase matching bandwidth for the noncollinear type-I interaction geometry; a single-pass configuration is used to maximize the gain bandwidth. The amplified pulses have energy of approximately 2 μJ and peak-to-peak fluctuations of less than 5%.

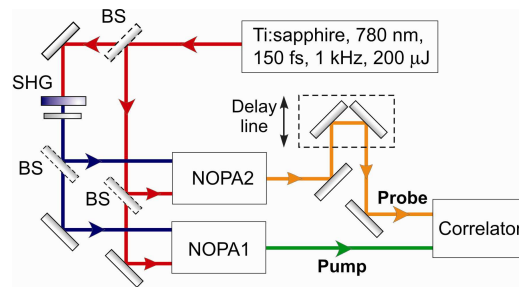


Figure 1: Block scheme of the experimental setup. BS: beam splitter. SHG: second harmonics generation. (redrawn from (**author?**) [3]).

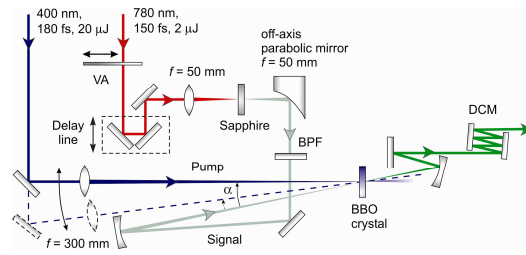


Figure 2: Setup of the noncollinear optical parametric amplifier. BPF: short pass filter that transmits only the visible part of the white light continuum and cuts out the fundamental and infrared components. (redrawn from (author?) [3]).

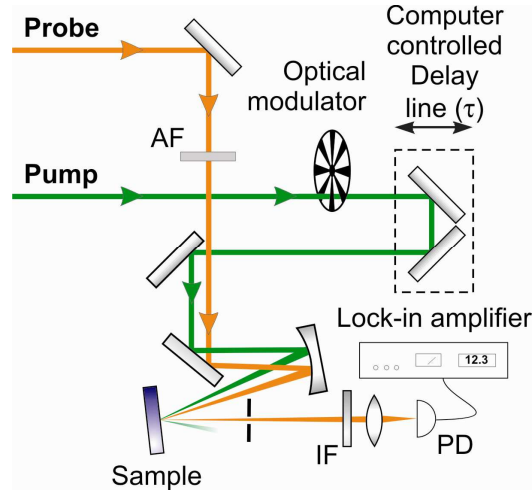


Figure 3: Schematics of the experimental apparatus used for auto/ cross-correlation and pump-probe experiments. AF: attenuating filter. IF: interference filter. PD: photodiode. (redrawn from (author?) [3]).

The compressor for the ultrabroadband NOPA consists of two custom-designed double-chirped mirrors (DCMs), manufactured by ion-beam sputtering (Nanolayers GmbH), which are composed of 30 pairs of alternating SiO₂ /TiO₂ quarter-wave layers in which both the Bragg wavelength and the layer duty cycle are varied from layer pair to layer pair. The DCMs introduce a highly controlled negative group delay (GD) over bandwidths approaching 200 THz, compensating for the GD of the NOPA pulses.

The narrower bandwidth NOPA providing the pump pulses is built identically to the one described above, only the amplified bandwidth is reduced by choosing a suitable non-optimum angle between pump and signal beams (dashed path of the blue pump in Figure 2). The pulses are compressed by DCMs similar to those used for the broadband NOPA.

A schematic of the apparatus used for pulse characterization and pump-probe experiments (correlator in Fig. 1) is shown in Fig. 3. The delay line is formed by two 90° turning mirrors mounted on a precision translation stage with 0.1 μm positioning accuracy (Physik Instrumente GmbH, model M-511.DD), which corresponds to 0.66 fs time resolution. The two pulses are combined and focused on the sample by a silver spherical mirror (R=200 mm). The non-collinear configuration enables to spatially separate pump and probe beams. Upon reflection from the sample, the probe beam is selected by an iris and steered to the detector, either a silicon photodiode preceded by a 10 nm spectral width interference filter or an optical multichannel analyzer (OMA). The differential reflection (transmission) signal is obtained via synchronous detection (lock-in amplifier Stanford SR830 for the photodiode, custom made software for the OMA) referenced to the modulation of the pump beam at 500 Hz by a mechanical chopper (Thorlabs MC1000). This allows detection of differential reflection ($\Delta R/R$) signals as low as 10⁻⁴.

C. Estimate of the electron-electron relaxation time

The applicability of the FL theory has been somewhat controversial in cuprate superconductors. The recent unambiguous observation of de Haas – van Alphen oscillations (author?) [5] has shown that the Fermi surface is almost cylindrical. In this quasi-two-dimensional case the electrons can be described as a FL if $r_s = a/a_B < 37$, with a being the mean electron distance and a_B the Bohr radius (author?) [6]. We determine $a = 1/\sqrt{n} = \sqrt{2\pi}/k_F$, with $k_F = 7.4 \text{ nm}^{-1}$ from (author?) [5]. Using $a_B = \hbar^2 \epsilon_{eff}/m^* e^2$, with $m^* = 4m_e$ and the effective dielectric constant $\epsilon_{eff} \approx 30$, we obtain $r_s \approx 1$, safely in the FL regime.

We can now use the FL theory to estimate the e-e relaxation time. In a FL the e-e relaxation time τ_{e-e} is given by : $1/\tau_{e-e} \approx \pi^3 \mu_c^2 (k_B T_e)^2 / 4\hbar E_F$ (author?) [7], where $\mu_c = r_s/2\pi$ is the Coulomb pseudopotential characterising the electron-electron interaction. Using $E_F = \hbar^2 k_F^2 / 2m^* = 0.5 \text{ eV}$ (author?) [5] and $T_e = 300 \text{ K}$, we obtain $\tau_{e-e} \approx 2.6 \text{ ps}$, which is much slower than our observed τ_a . In the main paper we give τ_{e-e} values for different T_e corresponding to different excitation fluences.

D. Exact relaxation rates

Here, differently from previous studies based on the two-temperature model (TTM), we analyze pump-probe relaxation rates using an analytical approach to the Boltzmann equation (author?) [8], which is free of any quasi-equilibrium approximation. Due to the complex lattice structure of cuprate superconductors characteristic phonon frequencies spread over a wide interval $\hbar\omega/k_B \gtrsim 200 \div 1000 \text{ K}$. Very fast oxygen vibrations with frequencies $\omega \gtrsim 0.1/f_s$ do not contribute to the relaxation on the relevant time scale, but just dress the carriers. For the remaining part of the spectrum we can apply the Landau-Fokker-Planck expansion, expanding the e-ph collision integral at room or higher temperatures in powers of the relative electron energy change in a collision with a phonon, $\hbar\omega/(\pi k_B T) \lesssim 1$. Then the integral Boltzmann equation for the nonequilibrium part of the electron distribution function $\phi(\xi, t) = f(\xi, t) - f_0(\xi)$ is reduced to a partial differential equation in time-energy space (author?) [8]:

$$\gamma^{-1} \dot{\phi}(\xi, t) = \frac{\partial}{\partial \xi} \left[\tanh(\xi/2) \phi(\xi, t) + \frac{\partial}{\partial \xi} \phi(\xi, t) \right], \quad (1)$$

where $f(\xi, t)$ is the non-equilibrium distribution function, and $\gamma = \pi \hbar \lambda \langle \omega^2 \rangle / k_B T$. The electron energy, ξ , relative to the equilibrium Fermi energy is measured in units of $k_B T$. Here $\lambda \langle \omega^2 \rangle$ is the second moment of the familiar Eliashberg spectral function (author?) [9], $\alpha^2 F(\omega)$, defined for any phonon spectrum as:

$$\lambda \langle \omega^n \rangle \equiv 2 \int_0^\infty d\omega \frac{\alpha^2 F(\omega) \omega^n}{\omega}. \quad (2)$$

The coupling constant λ , which determines the critical temperature of the BCS superconductors, is $\lambda = 2 \int_0^\infty d\omega \alpha^2 F(\omega) / \omega$.

Multiplying Eq.(1) by ξ and integrating over all energies yield the rate of the energy relaxation:

$$\dot{E}_e(t) = -\gamma \int_{-\infty}^\infty d\xi \tanh(\xi/2) \phi(\xi, t), \quad (3)$$

where $E_e(t) = \int_{-\infty}^\infty d\xi \xi \phi(\xi, t)$ and $\phi(\xi, t)$ is the solution of Eq. 1. Apart from a numerical coefficient the characteristic e-ph relaxation rate (proportional to γ) is about the same as the TTM energy relaxation rate (author?) [10], $\gamma_T = 3\hbar\lambda \langle \omega^2 \rangle / \pi k_B T$.

To establish the numerical coefficient we solved Eq.(1) and fitted the numerically exact energy relaxation by a near-exponential decay $E(t) = E_0 \exp(-at\gamma - bt^2\gamma^2)$, with the coefficients $a = 0.14435$ and $b = 0.00267$, which are virtually independent of the initial distribution, $\phi(\xi, 0)$ and pump energy, E_0 . The exact relaxation time $\tau = 1/a\gamma$ turns out longer than the TTM relaxation time γ_T^{-1} , by a factor of 2, (see Fig. 4), $\tau = 2\pi k_B T / 3\hbar\lambda \langle \omega^2 \rangle$. This as well as the shorter relaxation times observed in our ultra-fast pump-probe measurements lead to essentially higher values of EPI coupling constants compared with previous studies.

E. Exact transient electron distribution function

In the TTM e-e collision creates a quasi-equilibrium electron distribution that subsequently cools down via e-ph interaction and electron diffusion. On the other hand, in our relaxation scheme, which is dominated by e-ph

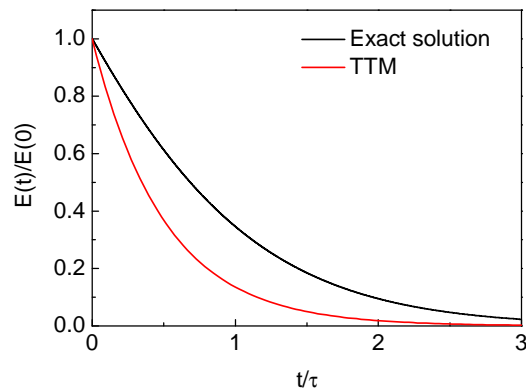


Figure 4: Numerically exact energy relaxation rate compared with TTM rate. E_0 is the pump energy, $\tau = 2\pi k_B T / 3\hbar\lambda\langle\omega^2\rangle$ is the exact relaxation time.

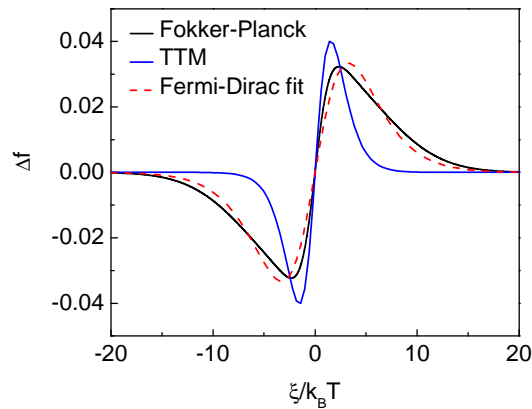


Figure 5: Difference $\Delta f = f(\xi, t = \gamma^{-1}) - f_0(\xi)$ of the transient distribution functions $f(\xi, t = \gamma^{-1})$ and the equilibrium Fermi-Dirac function $f_0(\xi)$. $f(\xi, t)$ is calculated from the Fokker-Planck equation and via the TTM, respectively.

interaction, the electron distribution during relaxation is not a quasi-equilibrium one. The *deviation* of both functions from the equilibrium is shown in Fig. 5, for $t = \gamma^{-1}$. Since we limit our discussion to the linear regime, the TTM correction to the distribution function is $\Delta f \propto x / \cosh(x^2/4)$, where $x = \xi/k_B T$. The width of the two lobes in Δf indicate the effective electronic temperature. The significantly narrower lobes for the TTM compared to the exact distribution illustrate how the TTM underestimates the transient electronic temperature and hence the relaxation time. However, the e-ph dominated relaxation is not just a slower relaxation through the same quasi-equilibrium states as assumed by the TTM. We illustrate this by fitting our non-equilibrium distribution with a quasi-equilibrium one (dashed line in Fig. 5). Since the Fokker-Planck equation describes diffusion in the energy space the high energy tails are clearly seen in our distribution, which, compared to the Fermi-Dirac distribution have a much gentler fall-off towards high electron energies.

While in the deviation from the equilibrium distribution, the difference between the two models is clearly visible, the Fermi-Dirac distribution and the one obtained from solving the Fokker-Planck equation, themselves look rather similar, except for the high energy tail, as can be seen in Fig. 6a. This shines new light on fs ARPES experiments, which directly measure the transient electron distributions. Until now it was customary to use the TTM to describe electron relaxation, ARPES data were in good agreement and were invoked as confirmation of the ultrafast e-e thermalization. We have now shown that a *similar* distribution can be obtained also as a result of e-ph scattering. In Fig. 6b we redraw the best available time-resolved ARPES data for cuprate superconductors (**author?**) [11] together with their fit to a quasi-equilibrium Fermi-Dirac distribution, from which they estimate a hot electron temperature. The spectrum was taken immediately after excitation (at the end of the pump-probe pulse overlap, which is about $\tau/2$ of their decay time after maximum pump-probe overlap, i.e. on average the electrons are probed $\tau/2$ after their excitation). Compared to the Fermi-Dirac curve, their data show a high-energy tail very similar to the exact non-equilibrium distribution we calculated. This means that our relaxation scheme is not only more justified than the TTM on the basis of the physical reasoning described in the main text, it also agrees better with experimental data in the

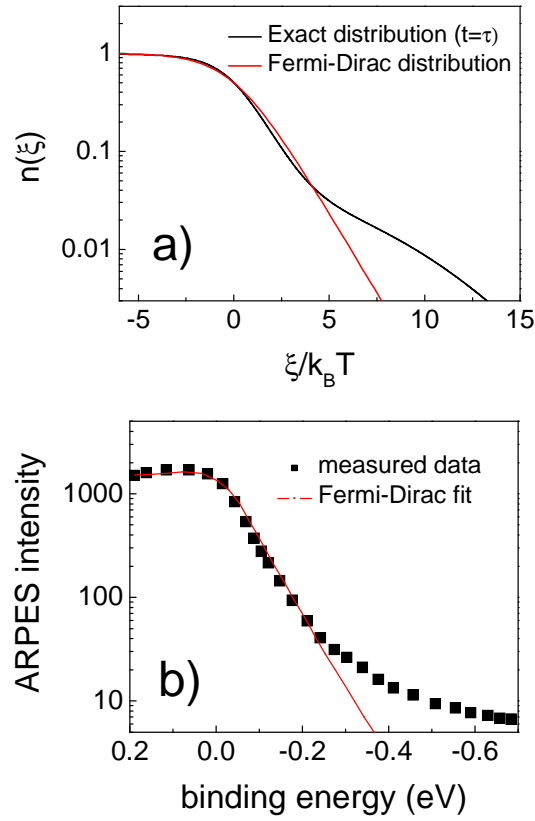


Figure 6: a) Numerically exact distribution function $f(\xi, t = \gamma^{-1})$ compared to a Fermi-Dirac distribution function with the same effective temperature. b) ARPES spectrum of $\text{Bi}_2\text{Sr}_2\text{CaCu}_2\text{O}_8$ immediately after excitation and fit to a Fermi-Dirac function (redrawn from (author?) [11]).

literature. This should in no way derogate the work done before our model was available, however, we propose to reassess quantitative conclusions along the lines of our relaxation scheme. Fortunately, the procedure to extract of $\lambda\langle\omega^2\rangle$ is qualitatively the same, only the obtained values should now be bigger by a factor of 2.

-
- [1] X. Yao, T. Mizukoshi, M. Egami, Y. Shiohara, *Physica C* **263**, 197 (1996).
 - [2] S. Sugai, H. Suzuki, Y. Takayanagi, T. Hosokawa, N. Hayamizu, *Phys. Rev. B* **68** 184504 (2003).
 - [3] C. Manzoni, D. Polli, G. Cerullo, *Rev. Sci. Instrum.* **77**, 023103 (2006).
 - [4] G. Cerullo, S. De Silvestri, *Rev. Sci. Instrum.* **74**, 1 (2003).
 - [5] B. Vignolle *et al.*, *Nature* **455**, 952 (2008).
 - [6] B. Tanatar and D. M. Ceperley, *Phys. Rev. B* **39**, 5005 (1989).
 - [7] See, for example N. W. Ashcroft and N. D. Mermin *Solid State Physics* (Harcourt, Orlando, 1976).
 - [8] V. V. Kabanov, A. S. Alexandrov, *Phys. Rev. B* **78** 174514 (2008).
 - [9] G. M. Eliashberg, *Zh. Eksp. Teor. Fiz.* **38**, 966 (1960); **39**, 1437 (1960) [*Sov. Phys. JETP.* **11**, 696; **12**, 1000 (1960)].
 - [10] P. B. Allen, *Phys. Rev. Lett.* **59**, 1460 (1987).
 - [11] L. Perfetti, *et al.*, *Phys. Rev. Lett.* **99**, 197001 (2007).